JOURNAL OF APPLIED ELECTROCHEMISTRY 21 (1991) 588–596

Electrochemical oxidation of sulphite ions at graphite electrodes

T. HUNGER, F. LAPICQUE, A. STORCK

Laboratoire des Sciences du Génie Chimique, CNRS-ENSIC-INPL 1, rue Grandville, B.P. 451, F-54001 Nancy Cedex, France

Received 26 February 1990; revised 28 November 1990

The electrochemical oxidation of sodium sulphite has been studied in aqueous sodium sulphate solution at two different graphite electrodes, one being of natural graphite (EC) and the other impregnated with phenol (ECK). The objective of the present work was to obtain some insight into the direct oxidation as well as the indirect oxidation, via produced oxygen radical species, of sulphite on non-metal electrodes. For this reason a study of the oxidation of sulphite in the concentration range between 0–0.10 M in aqueous sodium sulphate using a batch electrochemical reactor, operating potentiostatically, was undertaken. The potential range was chosen between 1.0 to 2.5 V/SCE, and the concentration of the supporting electrolyte, sodium sulphate, was kept constant at 0.5 M. A kinetic Tafel type law, considering irreversible behaviour for the direct sulphite oxidation and the mass transfer performance in regards to the experimental conditions were applied to predict the time variations of the sulphite conversion.

Notation

A_e	area of electrode (m^2)
a_e	specific area of electrode (m^{-1})
c_i	concentration of species i (M or $mol\,m^{-3}$)
D	diameter of impeller (m)
$\mathbf{D}$	diffusion coefficient ($m^2\,s^{-1}$)
E	electrode potential (V)
e	distance between the two eccentric tubes (m)
E_0	equilibrium potential (V)
E_0^0	standard potential (V)
F	Faraday constant ($=96\,485\,A\,s\,mol^{-1}$)
f	ratio (F/RT) (V^{-1})
i	current density averaged on the geometrical electrode surface ($A\,m^{-2}$)
I	total current (A)
i_k	kinetically limited current density ($A\,m^{-2}$)
i_{lim}	limiting current density ($A\,m^{-2}$)
i_0	exchange current density ($A\,m^{-2}$)
i_{00}	specific exchange current density defined by Equation 11
k_d	average mass transfer coefficient ($m\,s^{-1}$)
K_w	ionic product of water (M^2)
L	characteristical length (m)
m	molality ($mol\,kg^{-1}$)
n	order of the electrochemical reaction, defined by Equation 11
n	number of moles
N	stirring rate (r.p.s.)
Q'	heat flow rate (W)
Q_i	charge passed for time segment i (A s)
Q_{max}	maximal charge consummable during electrolysis (A s)
R	gas constant ($8.314\,J\,mol^{-1}\,K^{-1}$)
S	form factor defined by Equation 17
r_1, r_2	radius of electrodes
T	temperature (K)
X_A	conversion term of species A
V_l	liquid volume of the reactor (L or m^3)

Dimensionless numbers

Re	Reynolds number, defined as (ND^2/v)
Sc	Schmidt number, defined as ($v/\mathbf{D}$)
Sh	Sherwood number, defined as ($k_d D/\mathbf{D}$)

Greek letters

α	charge transfer coefficient
β	exponent used in Equation 21
γ	activity coefficient
η	overpotential (V)
κ	specific conductivity ($\Omega^{-1}\,m^{-1}$)
λ	thermal conductivity ($W\,m^{-1}\,K^{-1}$)
μ	dynamic viscosity (Pa s)
ν	kinematic viscosity ($m^2\,s^{-1}$)
ν_e	number of electrons involved
ρ	specific gravity ($kg\,m^{-3}$)
Φ_e	current efficiency

Subscripts

A	compound A
b	bulk
e	electrode
ferri	relative to ferri/ferro system
sulphite	relative to the sulphite/sulphate system
0	initial condition

0021-891X/91 $03.00 + .12

1. Introduction

1.1. *Oxidation of sulphite*

Several redox systems of sulphur are irreversible, which means that the potential of an inert electrode immersed in a solution containing both the oxidized and reduced forms is generally not stable with time and exhibits a behaviour not corresponding to that expected by the Nernst equation. For example, the sulphite–sulphate as well as the sulphite–dithionate systems are irreversible [1–3].

Sulphate and dithionate are formed during the oxidation of sulphite in alkaline and neutral solutions. Since the electrolytic oxidation of sodium sulphite to sodium sulphate Na_2SO_4 and to sodium dithionate $Na_2S_2O_6$, are electrolytically irreversible, no diaphragm is needed [4]. Hydrogen is evolved at the cathode during the electrolysis of alkaline solutions of sulphite (pH > 7), but SO_3^{2-} anions are not reduced [5]. The possible reactions occurring at the anode and cathode are listed below, where the standard equilibrium potentials were calculated using reliable values of Gibbs energies [5].

(i) *anode*

$$SO_3^{2-} + 2OH^- \longleftrightarrow SO_4^{2-} + 2e^- + H_2O \qquad E_0^0 = -0.936\,\text{V/NHE} \qquad (1)$$

$$2SO_3^{2-} \longleftrightarrow S_2O_6^{2-} + 2e^- \qquad E_0^0 = 0.037\,\text{V/NHE} \qquad (2)$$

At higher potentials the onset of oxygen is possible with the overall reaction in alkaline solution being

$$4OH^- \longleftrightarrow O_2 + 2H_2O + 4e^- \qquad (3)$$

The equilibrium potential of the oxygen redox electrode can be calculated from the Nernst equation depending on pH-range, water and hydroxide activity as well as the partial pressure of oxygen. The values of these potentials are of a limited significance since sulphite and dithionate species are metastable in aqueous solutions and much higher potential should be required for oxidations in Equations 1 and 2.

(ii) *cathode*

At the cathode only the evolution of hydrogen occurs from the dissociation of water. The potential of the H_2/H^+ couple in pure water and in molar hydroxide solution can be calculated from the Nernst equation and the ionization constant of water at 298.15 K:

$$H_2O \longleftrightarrow H^+ + OH^- \qquad K_W = 1.27 \times 10^{-14}\,M^2 \qquad (4)$$

$$2H_2O + 2e^- \longleftrightarrow H_2 + 2OH^- \qquad E_0^0 = -0.828\,\text{V/NHE} \qquad (5)$$

The amount of dithionate produced at the anodic surface was shown to depend on operating conditions, namely anode material, its preparation, current density, solution pH and presence of additives in the electrolyte solution [6, 7]: for instance, dithionate yields up to 30% can be obtained on nickel or gold electrodes, whereas this yield does not exceed 3% for graphite electrodes.

Of many mechanisms put forward for the oxidation of sulphite on metal electrodes in neutral and alkaline solutions, two seem the most plausible: the electrochemical mechanism involving slow loss of the first electron, and the mechanism postulating the participation of an oxide layer formed on the electrode surface [7]. Nevertheless, the validity of these mechanisms has to be clarified in the case of non-metal electrodes.

1.2. *Potential and thermodynamics of the sulphite cell*

With use of Equation 1, the Nernst equation for the oxidation of sulphite to sulphate can be written as

$$E = E_0^0 + \frac{RT}{2F} \ln \left[\frac{a_{SO_4^{2-}}}{a_{SO_3^{2-}} [a_{OH^-}]^2} \right] \qquad (6)$$

Furthermore, defining the activity coefficients as $a_i = m_i \times \gamma_i$ the liquid phase concentrations were expressed in molality, and with the use of the ionization constant of water at 298.15 K, Equation 6 may be rewritten as

$$E_0 = E_0^0 + \frac{RT}{2F} \times \left[\ln \left(\frac{1}{K_W^2} \right) + \ln \left(\frac{m_{SO_4^{2-}} \gamma_{SO_4^{2-}} [m_{H_3O^+} \times \gamma_{H_3O^+}]^2}{m_{SO_3^{2-}} \gamma_{SO_3^{2-}}} \right) \right]$$

By applying the definition of $pH = -\log (a_{H^+})$ and by use of the fact that the activity coefficients of SO_3^{2-} and SO_4^{2-} are approximately of the same order [8], one obtains finally for the equilibrium potential $E_{0/SCE}$ (refered now to the saturated calomel: $\Delta E = -0.2438$ V) as a function of pH and of the existing molalities of the species. Thus,

$$E_{0/SCE} = -0.3578\,\text{V} + 0.0296 \left[\log \frac{m_{SO_4^{2-}}}{m^{SO_3^{2-}}} - 2\,\text{pH} \right] \qquad (7)$$

1.3. *Graphite electrodes*

Evolution of a mixture of gases containing O_2, CO and CO_2 may take place at the surface of carbon and/or graphite anodes [9], when anodically polarized in a supporting electrolyte solution. The mechanism of formation of these gaseous substances has not yet been clarified; however, most studies mention the anodic charge transfer of H_2O or OH^- prior to gas evolution. Electrode-impedance measurements of gas evolution showed high values for the exchange-current densities, meaning that the oxygen overvoltage was mainly a concentration overvoltage. At low cur-

rent densities an adsorption overvoltage was found to predominate, changing to a predominant diffusion overvoltage with increasing current density. Furthermore at high potentials ($E > 2.0$ V) and high exchange current densities, a CO_2 yield (up to 40%) could be observed, corresponding to an inhibition of electron transport and a destruction of the graphite lattice [11]. The following mechanism can be considered on a graphite electrode:

$$OH^- - e^- + C \longleftrightarrow C\text{–}OH_{ads} \quad (8)$$

$$C\text{–}OH_{ads} + OH^- - e^- \longleftrightarrow C + H_2O + \tfrac{1}{2}O_2 \quad (9)$$

Furthermore it is known that the chemical nature of the particle discharge, OH^- or H_2O, is described to govern the chemical composition of the gas produced and the Tafel parameter, b, for the overall process [11]. Thus three regions can be distinguished on the curve of the gas composition against pH at current densities in the range 10–100 A m^{-2} [11, 12]: (i) for pH below 7, b is roughly constant at 0.2 V (decade)$^{-1}$ and CO_2 predominates in the gas generated; (ii) in neutral or weakly alkaline solutions, the extent of graphite combustion decreases, accompanied by significant decrease in the Tafel parameter; (iii) The discharge of the OH^- ion, observed in a strong alkaline pH range, corresponds to quantitative O_2 evolution; the b value is reported to be to 0.06 V (decade)$^{-1}$.

The study of the direct/indirect electrochemical oxidation of the sulphite ion on graphite materials has been little investigated. In the early sixties, Shlygin *et al.* [13] demonstrated that the oxidation at a platinum electrode could not be due to direct electron transfer but was due to the discharge of oxygen or other reactive species. The exact mechanism of the oxidation at a graphite electrode has not yet been elucidated.

2. Experimental details

2.1. *The setup*

Figure 1 shows a schematic diagram of the experimental apparatus. The vessel used in this study was a continuous stirred electrochemical tank reactor (CSTER) equipped with a water jacket having a volume close to 500 cm^3 and an internal diameter of 7.6 cm. The reactor was equipped with one acrylic-resin flat-blade Rushton impeller ($D = 3.6$ cm) with 6 vertical blades supported on a disc and was mounted at 1/3 of the liquid height from the bottom. Precise control of rotation speed was ensured by an electric motor controlled by a digital optical tachometer.

The experimental operating conditions were: (i) batchwise, (ii) stirring speed = 500 r.p.m., (iii) at $T = 298.1 \pm 0.1$ K, and (iv) at atmospheric pressure.

2.2. *Electrodes*

The cell for the potentiostatic studies was a conventional three-electrode arrangement. The working electrodes were of rectangular shape, 5 cm × 1.35 cm × 1.0 cm, corresponding to a geometrical area of 24.85 cm^2.

Two graphite materials were used in the present study. Both were supplied by Deutsche Carbon A.G., Frankfurt/Main, FRG. One graphite, denoted EC, was natural graphite non-impregnated. The other graphite, ECK, was prepared by impregnation in phenolic resin solutions at 400° C. The specific gravities of the graphites used were 1670 and 1940 kg m^{-3} for the EC and ECK grades, respectively. Specific areas estimated by the BET-method (CO_2 adsorption), were found to be 34 m^2 g^{-1} and 20 m^2 g^{-1} for the EC and ECK grades, respectively. Porosity and pore size determination were measured by mercury intrusion

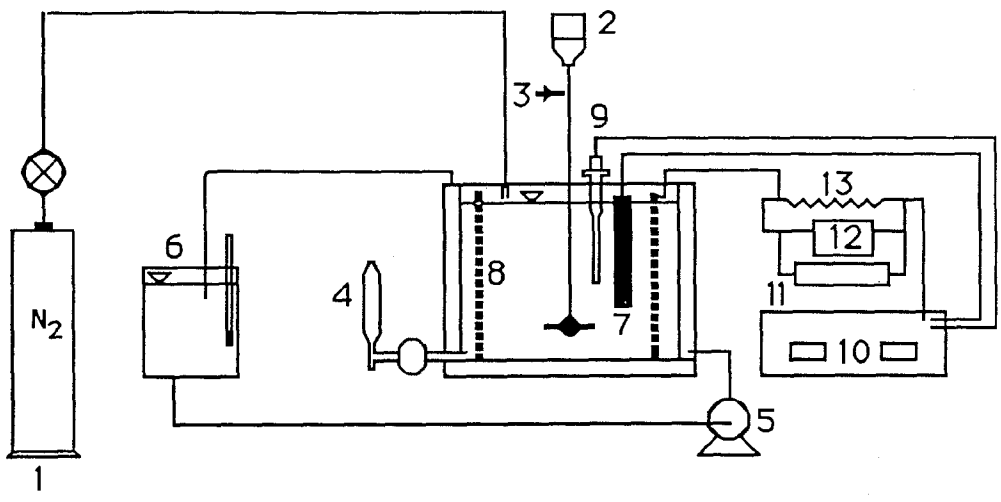

Fig. 1. Experimental apparatus: (1) nitrogen cylinder; (2) constant speed motor; (3) agitated vessel; (4) sampling pipette; (5) liquid circulating pump; (6) storage tank with constant temperature control unit; (7) working electrode; (8) counter-electrode; (9) reference electrode; (10) potentiostat; (11) recording instrument; (12) voltmeter; (13) variable ohmic resistance.

(Porosimeter 2000 Carlo Erba Strumentazione): as expected, larger value porosity was obtained for EC graphite (21%) compared to 9.4% for ECK graphite.

The potential of the working electrode was fixed at the required level with a scanning potentiostat (Model 361 Princeton Applied Research). A Tacussel calomel reference electrode was used in conjunction with a salt bridge tube filled with a saturated solution of potassium chloride. The counter electrode consisted of a comparatively large cylindrical sheet of expanded platinized titanium having a wetted area of approximately 350 cm^2. The real or wetted area was determined with an accuracy of about 5% from the external geometrical dimensions of the sheet and the intrinsic parameters of the mesh used [14].

The graphite electrodes were operated in the fully-immersed condition. The test electrodes were not pretreated or anodically polarized prior to an experimental run. After each run they were removed from the solution, cleaned in hot water, rinsed with distilled water and dried. Measurements of pH were made with a pH-glass electrode (Metrohm 632) directly before and after each experimental run.

2.3. *Reagents and analytical*

All chemicals were reagent grade and were used without further purification. The distilled water used in the experimental runs was filtered beforehand through microporous filter cartridges (Millipore S.A France) (d_{pore} = 0.22 μm) having a final resistivity of 18 MΩ cm. Prepurified grade nitrogen was used to deoxygenate the 0.5 M Na_2SO_4 electrolyte solution just prior to the introduction of sulphite. The concentration of sulphite was varied from 10^{-2} up to 0.1 M and the pH of the solutions was in the range 9.0–9.2. During test runs the solutions were blanketed with nitrogen. The amount of sulphite oxidized during the experimental runs was determined as a function of the time by analysing the liquid. Samples were withdrawn from the bottom of the vessel at regular time intervals (60 min). The sulphite ion concentration was determined by adding an excess of a standard iodine solution followed by back titration with a standard thiosulphate solution [15].

3. Kinetics of the oxidation

The kinetics of sulphite oxidation were studied using linear voltammetry at a rotating disc electrode [16]. Typical *i–E* plots are shown in Fig. 2. For the two graphite materials tested, the *i–E* curves give a rise in current at about 0.2 V/SCE and current density gently increases with electrode potential; a weakly established current density plateau is first observed in the range 0.5–0.7 V/SCE, followed by a second rise in current density. A better defined plateau can be seen between 1.1 and 1.4 V/SCE, especially for low rotation rates. The onset of oxygen starts readily at 1.5 V.

The *i–E* plots were modelled by the simple Butler-Volmer law for irreversible direct process even though

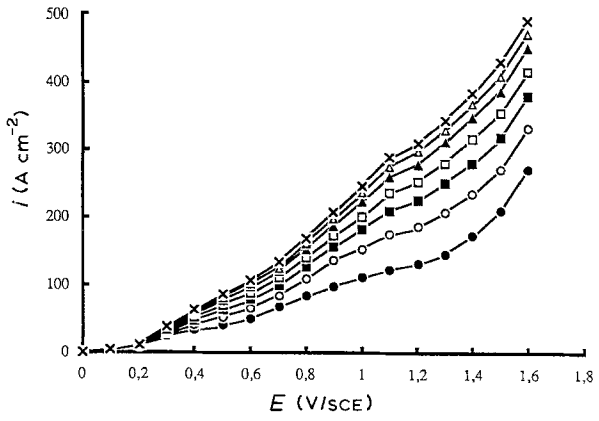

Fig. 2. Current density against applied potential for a natural graphite (EC) disc rotating at various speeds in aqueous 0.019 M Na_2SO_3 solution containing 0.5 M Na_2SO_4 at 25° C. Speeds: (●) 500, (○) 1000, (■) 1500, (□) 2000, (▲) 2500, (△) 3000 and (×) 3500 r.p.m.

the oxidation scheme has not been yet elucidated. The current density of sulphite oxidation was therefore characterized by the coefficient diffusion, **D**, and the kinetically limiting current density, i_k. The accurate procedure for determining the numerical values is described in a companion paper [16].

The values for diffusion coefficient, **D**, were corrected for migration phenomena; the contribution of migrational effects was calculated from the chemical composition of the bulk electrolyte. The values for **D** obtained for both electrode materials, were found to obey a decreasing function of the sulphite concentration within 10% [16]:

$$\mathbf{D} = (7.6 - 0.9 \times 10^{-2}[SO_3^{2-}]) \times 10^{-10}\ m^2\ s^{-1} \quad (10)$$

where $[SO_3^{2-}]$ is expressed in mol m^{-3}. In addition, Relation 10 was shown to be in excellent agreement with the theoretical expressions for **D** based on the analysis of the various electrostatic effects and the relaxation phenomena [17, 18]. As regards electrode kinetics, it was demonstrated that i_k could be expressed as a power function of the sulphite concentration with a constant α value: *viz*

$$i_k = i_0 \exp(\alpha v_e f\eta) = i_{00}[SO_3^{2-}]^n \exp(\alpha v_e f\eta) \quad (11)$$

where i_0 is the exchange current density. As shown in Table 1, the two kinds of graphite investigated exhibit different electrochemical behaviour: the ECK gives a larger current density in comparison with EC but a lower charge transfer coefficient. In addition the order of the electrode reaction seems too dependent on the material used but does not differ too much from unity. For the example of the oxidation of a 0.05 mol dm^{-3}

Table 1. Results of the numerical treatment of the experimental curves i–E [16]

Graphite	i_{00} ($A\,m^{-2}\,mol^{-n}\,m^{3n}$)	*n*	α
EC	0,0196	0.68	0.058
ECK	0,0070	1.34	0.048

sulphite solution at 1.1 V/SCE, the kinetically limited current density for ECK is twice as large as the one for the natural graphite EC.

4. Analysis of an electrochemical batch reactor

Considering the reaction occurring at the working electrode

$$SO_3^{2-} + 2OH^- \longleftrightarrow SO_4^{2-} + 2e^- + H_2O$$

the mass balance with respect to the reacting species A (SO_3^{2-}) in the batch reactor can be expressed as

$$\frac{dn_A}{dt} + \frac{1}{v_e F} = 0 \qquad (12)$$

In the general case of mixed control, the ratio of the concentrations of sulphite in the bulk of the solution as to that at the surface of the electrode can be written in the following manner

$$\frac{C_{Ae}}{C_{Ab}} = \frac{i_{lim} - i}{i_{lim}} \qquad (13)$$

where the limiting current is equal to $(v_e F k_d C_{Ab})$. These terms can be combined with Equation 12, supposing that initial concentration of the species A is $C_{A0} = n_{A0}/(V_l)$, to give the following first-order ordinary differential equation:

$$\frac{dC_{Ab}}{dt} = \left(\frac{-a_e}{v_e F}\right) \frac{i_{lim} i_0 \exp\left(\frac{\alpha v_e F}{RT}\eta\right)}{i_{lim} + i_0 \exp\left(\frac{\alpha v_e F}{RT}\eta\right)} \qquad (14)$$

The theoretical values for the concentration of sulphite as well as for the current density were numerically solved by use of a Runga-Kutta method for the solution of initial-value problems. As explained previously, the value for η was deduced from the measured electrode potential, taking into account the ohmic drop between the graphite slab and the reference electrode, and the rest potential, which could be calculated as a function of the sulphite concentration using Relation 7; the ohmic contribution relevant to the actual reactor was estimated by a technique described later.

By introducing the conversion factor X_A (having a value between 0 and 1) defined by the following relationship

$$X_A = \frac{n_{A0} - n_A}{n_{A0}} \qquad (15)$$

it was possible to compare the experimental values for the conversion factor to those theoretically calculated.

4.1. *Ohmic drop in the reactor: primary current distribution*

In the present study, as the working electrode was placed in an eccentric position to the counter electrode, the total primary current, I, was determined by applying the electrical field theory with the help of an analogy with heat conduction between two eccentric tubes of infinite length [19]. The analysis presented below is of limited physical meaning because of two phenomena: (i) the top and bottom of the electrodes are the source of edge effects in the current distribution; (ii) due to the large values of the overpotential, only tertiary distribution should be considered in a rigorous approach – due to the low electrode activation, the partial control from diffusion phenomena and the presence of gas bubbles, the actual distribution is likely to be more uniform than the primary distribution. Nevertheless, the simple approach used could yield approximate relations for the current distribution in the reactor.

The flow of heat from one isothermal area A_1 to another isothermal area A_2 of any geometrical arrangement can be calculated as follows:

$$Q' = -\lambda \iint (\partial T/\partial n)_1 dA_1 = -\lambda \iint (\partial T/\partial n)_2 dA_2 \qquad (16)$$

where n is the normal direction to the surface A_i. In practice a form factor, S, is introduced, which is defined as follows:

$$S = (T_2 - T_1)^{-1} \iint (\partial T/\partial n)_1 dA_1 = -(T_2 - T_1)^{-1} \iint (\partial T/\partial n)_2 dA_2 \qquad (17)$$

For various geometrical arrangements form factors have been calculated. For the case of two eccentric tubes of infinite length this leads to the following term:

$$S = \frac{2\pi}{\operatorname{arcosh}\left(\frac{r_1^2 + r_2^2 - e^2}{2r_1 r_2}\right)} \qquad (18)$$

The total primary current distribution term is now

$$I = \frac{\kappa \Delta E 2\pi L}{\operatorname{arcosh}\left(\frac{r_1^2 + r_2^2 - e^2}{2r_1 r_2}\right)} \qquad (19)$$

where ΔE is the cell voltage. By anology between the area of the graphite slab, being of cubic form, to the equivalent area of a supposed electrode, now of cylindrical form, the radius r_1 was calculated. The characteristical length, L, the radius, r_2, of the counter electrode, as well as the eccentric distance, e, were taken from the experimental set-up.

5. The estimation of mass transport coefficient

The diffusion controlled electrochemical technique used in this study was the reduction of potassium ferricyanide to potassium ferrocyanide at a nickel electrode having the same dimensions as the graphite electrodes. The solutions were: (i) 1 N NaOH; (ii) 0.1 M potassium hexacyanoferrate (II), $K_4[Fe(CN)_6] \cdot 3H_2O$; (iii) 5×10^{-3} M potassium hexacyanoferrate (III), $K_3[Fe(CN)_6] \cdot 3H_2O$. The mass transfer coefficients were determined by the electrochemical technique at different stirring speeds. Plotting k_d against N

in a double logarithm chart shows a good linearity and gives:

$$k_{d,ferri} = 2.9 \times 10^{-7} Re^{0.65} (m\,s^{-1}) \quad (20)$$

where Re is the Reynolds number of the stirred vessel. Relation 20 obtained with the ferri/ferro system, can be derived for the present case of sulphite oxidation, using dimensionless analysis $Sh = f(Re, Sc)$. Thus, for a given value of the stirring rate, N, the mass transfer coefficient related to the sulphite medium, $k_{d,sulphite}$, can be expressed as

$$k_{d,sulphite} = k_{d,ferri} (\mathbf{D}_{sulphite}/\mathbf{D}_{ferri})^{2/3} (\nu_{sulphite}/\nu_{ferri})^{1/3-\beta} \quad (21)$$

where β is the exponent appearing in Relation 20, equal to 0.65 in the present case. The viscosity of the electrolyte solutions were measured at 25° C with help of an Ubbelohde viscometer: ν_{ferri} was found to be equal to $1.091 \times 10^{-6}\,m^2\,s^{-1}$, in good agreement with the empirical relationship proposed in [20]. The viscosity of 0.5 M Na_2SO_4 containing solutions was observed to be slightly increased by the presence of sodium sulphite:

$$\nu_{sulphite} = (1.038 + 0.371 \times 10^{-3}[SO_3^{2-}]) \times 10^{-6}\,m^2\,s^{-1} \text{ in the range } 0\text{–}100\,mol\,m^{-3} \quad (22)$$

where the sulphite concentration is expressed in $mol\,m^{-3}$. The diffusion coefficient of ferricyanide ion was estimated from the relationship of Bazan and Arvia [21]:

$$(\mathbf{D}_{ferri}\mu/T) = 2.52 \times 10^{-15} (m^2.\,Pa.\,K^{-1}) \quad (23)$$

Due to Relations 10 and 22, Relation 21 yielded values for $k_{d,sulphite}$ dependent on the sulphite concentration and on the reaction time, as a consequence. However, for an initial sulphite concentration of 0.05 M, the time variation of the mass transfer coefficient was estimated to 2.14% and average diffusion and mass transfer coefficients were therefore used for further investigations.

Gas bubbles occur for the highest potential values and induce an enhancement in mass transport at the electrode; however, no available data could be used for the particular cell geometry and this phenomenon, which can be of a major importance in the case of laminar flow [22], was not taken into account in the model.

6. Experimental results

During the electrochemical reaction at various sulphite concentrations the measured electrolysis current was recorded as a function of the time. From the potentiostatic data the charge passed through the reactor at designated time intervals, denoted as Q_i, was compared to the maximal amount of charge consummable during the electrolysis

$$Q_{max} = \nu_e F C_{A0} V_1 \quad (24)$$

The fraction of these two terms, the so-called reduced charge, was then compared with the corresponding conversion rate. All the following experimental runs were carried out for a duration of 7 h. Usually a sample volume of 5 cm^3 was taken from the reactor every sixty minutes. The amount of sulphite in each sample was determined twice by iodometry, and an average value of the two samples was taken. In order to ascertain more or less a constant reactor volume the 5 cm^3 taken from the reactor were replaced by 5 cm^3 of the supporting electrolyte, thereby maintaining on the one hand a constant reactor volume, yet on the other hand diluting to a certain extent the sulphite concentration. This dilution effect, however, was considered in the calculations of the variables used: the maximal charge, Q_{max}, the conversion, X, and also the current yield, Φ_e [17].

In the present study we investigated the influence of several parameters, namely the electrode potential, the electrode material and the sulphite concentration, on the conversion rate and the current yield. The reproducibility of the experiments presented was carefully checked.

6.1. *Influence of the electrode potential*

Figure 3 shows the conversion rate as a function of time for various potentials and an initial sulphite concentration of 0.046 ± 0.0035 M. Very similar results are observed for 'low' electrode potentials, i.e. 1.0 V and 1.2 V, corresponding to a mostly direct oxidation process. Increasing the potential over the limiting conditions allows the oxidation to be significantly enhanced (Fig. 3): for instance, at 2.5 V, the rate of conversion after 1 h was at 46.7% as compared to 18.8% for 1.2 V, which means an increase of 148%.

The measured current densities based on the geometrical surface of the graphite electrodes are reported against time in Fig. 4, for various operating conditions. The cell current is obviously a decreasing function of time during the batch oxidation, depend-

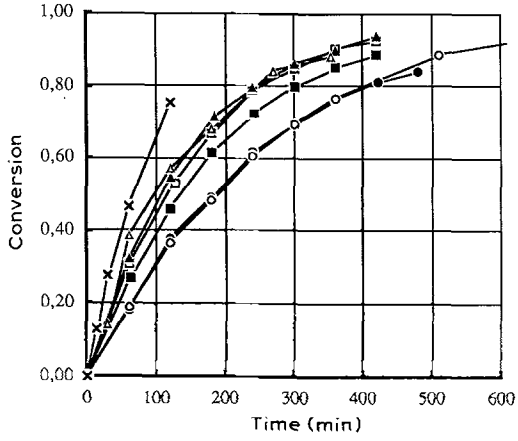

Fig. 3. Conversion rate of sulphite in dependance of electrolysis time for different working potentials with exact concentration values written in parentheses. All measurements were carried out at a constant concentration of 0.5 M Na_2SO_4 on non-impregnated graphite (EC) at 25° C. Key: (●) 1.0 V (0.0466 M); (○) 1.2 V (0.0425 M); (■) 1.4 V (0.0472 M); (□) 1.6 V (0.0474 M); (▲) 1.8 V (0.0473 M); (△) 2.0 V (0.0498 M); and (×) 2.5 (0.0446 M).

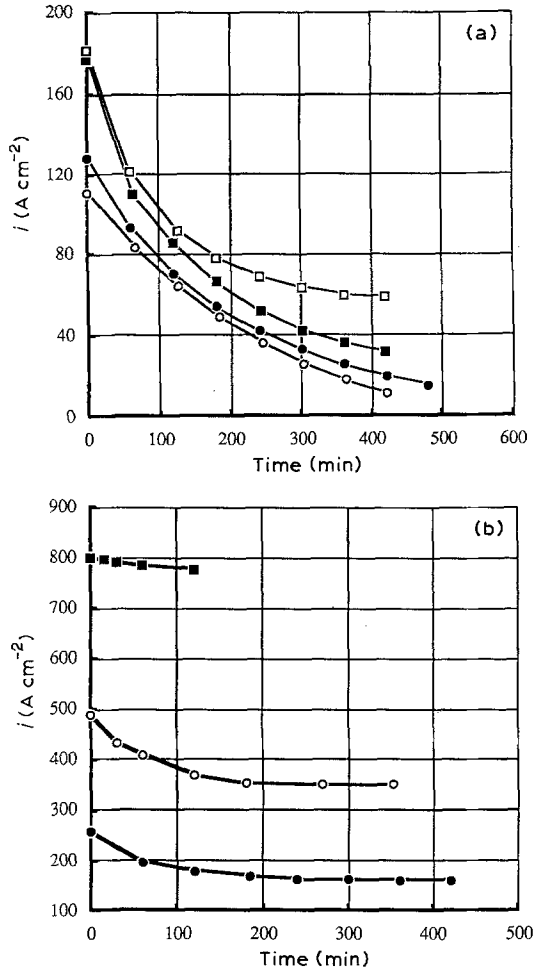

Fig. 4. Measured current densities for the oxidation of sulphite in dependance of electrolysis time for various potentials with initial concentrations of sulphite written in parentheses. All measurements were carried out at a constant concentration of 0.5 M Na_2SO_4 on non-impregnated graphite (EC) 25° C. Disc speed 500 r.p.m. Key for (a): (●) 1.0 V (0.0466 M); (○) 1.2 V (0.0425 M); (■) 1.4 V (0.0472 M); (□) 1.6 V (0.0474 M), and for (b): (●) 1.8 V (0.0473 M); (○) 2.0 V (0.0498 M); (■) 2.5 V (0.0466 M).

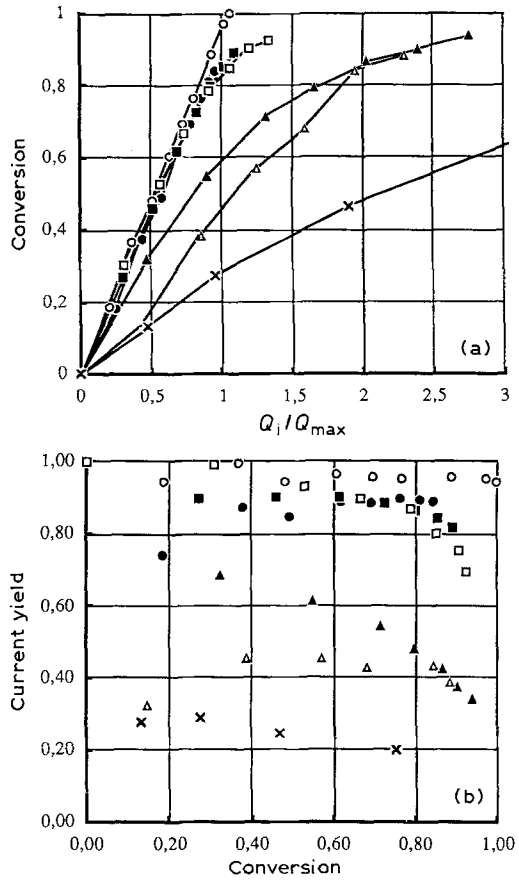

Fig. 5. (a) Conversion of sulphite ion in dependence with the reduced charge Q_i/Q_{max} for different working potentials. (b) Current efficiency in dependance with the conversion of sulphite ion for different working potentials. General conditions as in Fig. 4. Key for (a) and (b): (●) 1.0 (0.0466 M); (○) 1.2 V (0.0425 M); (■) 1.4 V (0.0472 M); (□) 1.6 V (0.0474 M); (▲) 1.8 V (0.0473 M); (△) 2.0 V (0.0498 M); and (×) 2.5 V (0.0446 M).

ing on the potential value. Actually, the current was observed to be increased by a rise in the electrode potential due to: (i) an increase in the kinetically limited current, which has a finite value for most cases; (ii) a possible bubble-induced enhancement in mass transport; and (iii) the onset of additional oxidative phenomena at the graphite surface such as gas evolution: this phenomenon seems to predominate at potential larger than 1.8 V/SCE.

Figure 5a shows the extent of conversion as a function of the reduced charge. Furthermore the current efficiency calculated is compared with sulphite conversion in Fig. 5b. It must be noted that the current yield was calculated on the basis of sulphite consumption and, for reasons given above, the formation of dithionate was neglected. Extremely high current efficiencies of up to 100% were noted for the measurements done at 1.0 V and at 1.2 V where the direct oxidation of sulphite on the graphite electrode was expected. The indirect process was shown to be quite efficient for moderate oxygen evolution as the current yield, measured at 1.6 V, was not reduced by the side electrode reacton put into evidence by the time variation of the current (Fig. 4a). However, the oxidative efficiency of the gas evolution was observed to be of a limited extent for higher potential values, as Φ_e measured after one hour, dropped from 94.4% for 1.2 V to 24.5% at 2.5 V.

6.2. *Influence of electrode material*

In order to investigate the performance of the two graphites considered during electrolysis, two experimental runs were carried out at a potential of 1.2 V (potential where the current efficiencies were high and direct oxidation of the sulphite species expected) for the two sorts of graphite. As can be seen from Fig. 6 the two graphites were found to exhibit similar behaviour. The rate of conversion of sulphite is slightly enhanced by use of graphite type EC, although the inverse was expected if one compare the kinetically limited current densities. The higher porosity of the graphite type EC may offer more active sites for the sulphite species tunneling their way into the porous lattice of the electrode during electrolysis. On the contrary, graphite ECK has a higher exchange current for most conditions, but may offer a much smaller active surface area in comparison to graphite EC.

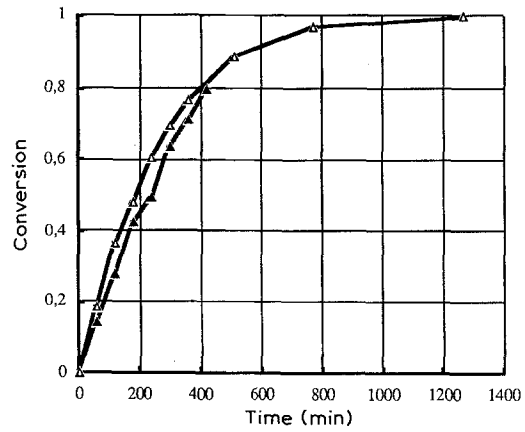

Fig. 6. Conversion rate of sulphite in dependance of the time of the electrolysis at a constant potential of 1.2 V on (△) non-impregnated artificial graphite (EC) and on (▲) artificial graphite impregnated with phenol (ECK). Note: concentration for EC (△) 0.0425 M and for ECK (▲) 0.0488 M. All measurements taken at 25° C and 500 r.p.m.

6.3. *Influence of the sulphite concentration*

The effect of sulphite concentration on the oxidation rate in the batch reactor was studied on an EC surface at 1.2 V/SCE, as shown in Fig. 7. Smaller amounts of sulphite ion were observed to be converted more rapidly. This result can be explained in a qualitative manner as follows: the comparison was done for a given value of working potential. Since the cell ohmic drop is an increasing function of the current density and thus of the sulphite concentration, the overpotential values calculated for initial conditions, are varied from 1.95 V at 0.0217 M down to 1.85 V at 0.093 M.

7. Comparison of experimental data with theory

In Fig. 8 the rate of conversion determined experimentally was compared to the theoretical rate of conversion calculated by numerical integration of the differential equation (14). As explained with Equation 14, incorporating the kinetic equation of

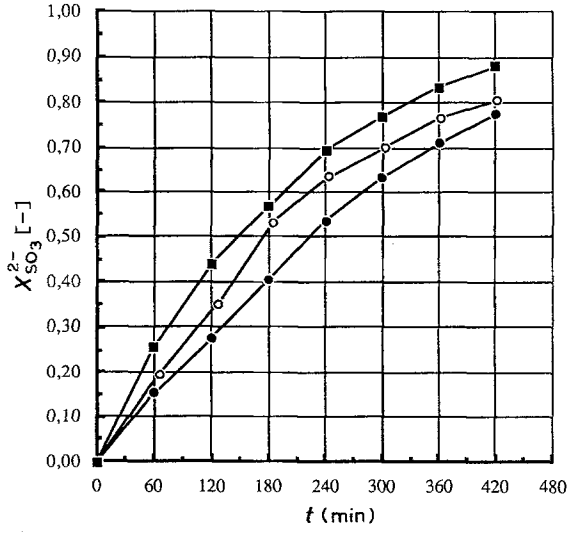

Fig. 7. Conversion rate of sulphite in dependance of the time of the electrolysis at a constant potential of 1.2 V: (Other conditions as in Fig. 4.) Key: (●) 0.093 M; (○) 0.0455 M; (■) 0.0217 M.

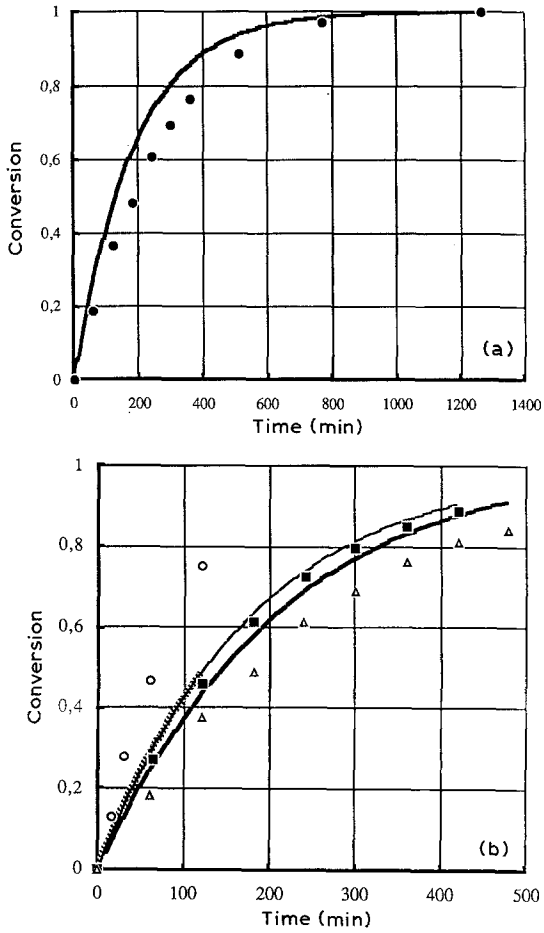

Fig. 8. Comparison of the experimentally determined conversion rate with the theoretical for the oxidation of sulphite against electrolysis time: (a) at 1.2 V/SCE (0.0425 M), (●) experimental, (——) theoretical. (b) at 2.5 V/SCE: (hatched line) theor. and (○) expt.; (0.0446 M); at 1.4 V/SCE: (——) theor. and (■) expt. (0.0472 M); and at 1.0 V/SCE: (——) theor. and (△) expt. (0.0466 M).

sulphite oxidation is only valuable when considering direct electrochemical oxidation with no gas evolution. At a potential of 1.2 V, a potential where the onset of gas evolution was negligible, the theoretical values are very consistent with the experimental. The discrepancies are very small and may be due to experimental error, side reactions (dithionate) and, perhaps, a small amount of gas production.

The validity of the theoretical results is shown clearly when comparing experimental results at three different potentials (Fig. 8b). It is noticed that, for a potential value of 1.0 V, the theoretical curve is slightly higher than the experimental one. At 1.4 V the experimental curve and the theoretical curve are identical and, in the range of significantly higher potential (E = 2.5 V), the strong onset of gas evolution causes a large difference in the experimental as well as the theoretical values.

Additionally, comparison was made with respect to current density. In accordance with the reasons stated above, in the region of mainly direct oxidation E = 1.0 V the discrepancies between predicted and experimental values are of minor order, as shown in Fig. 9. It was also observed that the experimental current densities were of magnitude greater than the theoretical calculated values for the highest applied

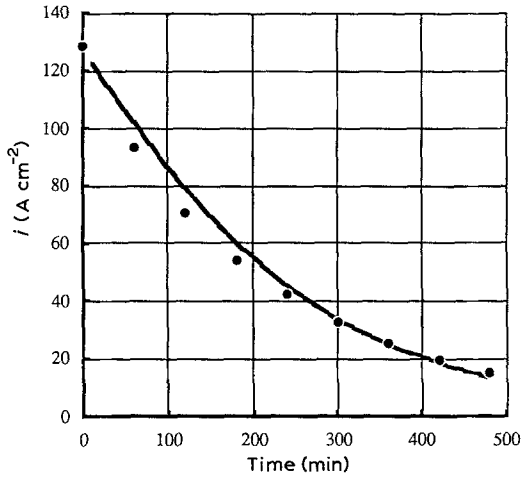

Fig. 9. Comparison of the experimentally determined current densities with the theoretical for the oxidation of sulphite at 1.0 V against electrolysis time. (●) 1.0 V (0.0466 M) and (——) theor.

voltage, due to the strong onset of gas evolution above 1.4 V.

8. Conclusion and significance

The present paper shows the feasibility of sulphite electrochemical oxidation on a graphite electrode as the oxidation can be completed with high current efficiency. Even though the sulphite ion oxidation cannot be considered as a simple and direct process and is known to involve oxidative intermediate species, the electrode reaction was characterized by an apparent diffusion coefficient and two kinetic coefficients, i_0 and α. The 'black-box' approach was used in order to describe the kinetic mechanism of the sulphite oxidation, which and was then, in turn, incorporated into the mass balance equation for a uniform batch reactor. This procedure allows satisfactory prediction of the electrochemical oxidation performance of the reactor for an electrode potential in the region, where no, or very little, gas evolution occurs. The deviation between theory and practice observed at higher potentials, is due to the parallel processes of direct electrochemical oxidation combined with gas evolvement and consequent electrode consumption.

Acknowledgments

The authors would like to thank Dr K. J. Müller of Deutsche Carbon A.G., Frankfurt/Main, FRG, for supplying the graphites used. The present work was sponsored by the Commission of the European Communities through the BRITE program (contract R I 1B-0223 C).

References

[1] G. N. Lewis, M. Randall and F. R. v. Bichowsky, *J. Am. Chem. Soc.* **40** (1918) 356.
[2] W. D. Bancroft and J. E. Magoffin, *ibid.* **57** (1935) 2561.
[3] J. Coursier, *Anal. Chim. Acta* **7** (1952) 77.
[4] W. D. Bancroft, *Trans. Electrochem. Soc.* **33** (1937) 195.
[5] A. J. Bard, R. Parsons and J. Jordan, 'Standard Potentials in Aqueous Solution', IUPAC (1985), Chapter 6, pp. 93–125.
[6] S. Glasstone and A. Hickling, *J. Chem. Soc.* (1933) 829.
[7] S. I. Zhdanov, in 'Encyclopedia of the Electrochemistry of the Elements', vol. 4 (edited by A. J. Bard), Marcel Dekker, New York (1975), p. 333.
[8] J. Kielland, *J. Am. Chem. Soc.* **59** (1937) 1675.
[9] F. Hine, M. Yasuda and M. Iwata, *J. Electrochem. Soc.* **121** (1974) 749.
[10] P. Drossbach and P. Schmittinger, *Electrochim. Acta* **11** (1966) 687.
[11] G. N. Kokhanov and N. G. Milova, in 'Modern aspects of electrochemistry', (edited by B. E. Conway, J. Bockris and P. E. White), Plenum Press, New York (1989) p. 315.
[12] L. I. Krishtalik and Z. A. Rotenberg, *Elektrokhimiya* **2** (1966) 351.
[13] G. L. Klyanina and A. I. Shlygin, *Russian Journal of Physical Chemistry* **36**(6) (1962) 692.
[14] C. Furiet, 'Surface réelle de métaux déployés', Internal report LSGC/GTREP (1985).
[15] J. H. Karchmer, 'The Analytical Chemistry of Sulfur and its Compounds' Part I, Wiley-Interscience, Chichester Eng. (1968).
[16] T. Hunger and F. Lapicque, to be published in *Electrochim. Acta.*
[17] T. Hunger, Internal Report, LSGC/GTREP (1989).
[18] P. Turq, R. Deloncle and M. Chemla, *J. Chem. Phys.* **68** (1971) 1305.
[19] VDI-Wärmeatlas 4, 'Stationäre Wärmeleitung', EA4-EA9, VDI Verlag GmbH, Düsseldorf (1984).
[20] S. L. Gordon, J. S. Newman and C. W. Tobias, *Ber. der. Bunsengesellschaft, Phys. Chem.* **70** (1966) 414.
[21] J. C. Bazan and A. J. Arvia, *Electrochim. Acta* **10** (1965) 1025.
[22] L. J. J. Janssen, *J. Applied Electrochem.* **17** (1987) 1077 and references cited therein.